Development and Modeling of Electrically Triggered Hydrogels for Microfluidic Applications

Michael J. Bassetti, Aveek N. Chatterjee, N. R. Aluru, *Member, IEEE*, and David J. Beebe, *Member, IEEE*

***Abstract*—In this paper, we present progress in the development of electrically triggered hydrogels as components in microfluidic systems. Stimuli-responsive hydrogels are fabricated using liquid-phase photopolymerization techniques and are subjected to different voltage signals in order to determine their volume change response characteristics. A chemoelectromechanical model has been developed to predict the swelling and deswelling kinetics of these hydrogels. The Nernst–Planck equation, Poisson equation, and mechanical equations are the basic governing relationships, and these are solved in an iterative manner to compute the deformation of the hydrogel in response to varied electrical input. [1019]**

***Index Terms*—Actuator, electrically triggered hydrogel, electric field, hydrogel, microfluidics, valve.**

I. Introduction

A LOOK at the current state of life science research reveals methods and protocols that have been more or less the same for decades. These protocols, for the most part, are cumbersome: a laboratory scientist spends hours mixing solutions in beakers, dispensing fluids drop by drop into microtiter plates, waiting for reactions to take place, and analyzing results by inspection or with the aid of expensive equipment. The field of microfluidics emerged primarily to improve on these time-intensive methods. The scaling down of conventional macroscale processes enables smaller sample volumes, less waste, higher throughput, improved efficiency and accuracy, and the potential for process automation. Indeed, many researchers think that microfluidics will be the key technology in revolutionizing the fields of medicine and biology, transforming them from the largely empirical sciences that they are presently into more mature and exact sciences.

As it stands, the field of microfluidics is still in its infancy. Far from being able to quickly transfer a technology from the macro- to the microworld, researchers in microfluidics are concerned primarily with developing the basic components with which to construct a whole system. Components like flow channels, pumps, valves, mixers, and sensors must be developed with the physics of the microscale in mind. Initially, researchers looked to use methods and materials used in semiconductor and microelectronics processing, but more and more are finding that these technologies are not adequate to create devices that can regulate and direct fluid flows. Because of the limitations of silicon, there is a trend toward engineering less conventional approaches to microfluidic system design [1], [2]. These alternative approaches often utilize processes that take advantage of the physics of the microscale (e.g., laminar flow or capillary action) and intelligent materials that sense and respond to the local fluid environment.

Stimuli-responsive hydrogels have been shown to be a natural choice for use in microfluidic systems because their response is controlled by diffusion processes. Hence, as hydrogel devices are made smaller, the time-response of their volume transitions becomes faster. Hydrogels have been shown to respond to a number of different stimuli, including pH [3], electric fields [4], temperature [5], light [6], and even organic compounds [7] and antigens [8]. Although responsive hydrogels have been studied extensively, their application has been limited by their slow response times at larger scales. Recently, however, many of these hydrogels have been receiving renewed attention as potential valves, filters, sensors, and actuators in microfluidic systems, where small (on the order of tens of μm) and fast (less than a second) responses are necessary.

In this paper, several methods of triggering hydrogel volume change with electrical signals are investigated. Generally speaking, this involves placing hydrogels near electrodes in a microchannel and applying different voltage signals. Depending on various environmental conditions, such as fluid composition, flow rate, nature of voltage signal, and the geometry and placing of the electrodes and hydrogels, different volume change responses will be seen. Among the benefits of electrical control is improved time response of volume change as compared to other means of hydrogel control and the ability to actuate individual hydrogels externally, independently, and repeatably. Ultimately, we believe that these hydrogels could prove useful as a high-speed valve or actuator in a range of microfluidic systems.

II. Background

The electrical triggering of hydrogel volume change has been reported in the literature for many years. Since as early as the 1960s there has been interest in applying this mode of control to hydrogels in applications ranging from robotic or prostheses

Manuscript received March 11, 2003; revised November 2, 2004. This work was supported under a Grant from DARPA (F30602-00-1-0570). Subject Editor Y.-C. Tong.

M. J. Bassetti is with the Department of Electrical and Computer Engineering, at the University of Wisconsin-Madison, Madison WI 53706 USA.

A. N. Chatterjee and N. R. Aluru are with the Beckman Institute for Advanced Science and Technology, University of Illinois at Urbana-Champaign, Urbana, IL 61801 USA.

D. J. Beebe is with the Department of Biomedical Engineering at the University of Wisconsin-Madison, Madison WI 53706 USA (e-mail: dbeebe@engr.wisc.edu).

Digital Object Identifier 10.1109/JMEMS.2005.845407

muscle to drug-delivery control membranes [9], [10]. Most experiments to date, however, are investigations into the basic properties of hydrogel response, and few if any true applications currently exist.

A. Previous Experiments

In 1965, Hamlen *et al.* reported that a poly(vinyl alcohol;VA)-poly(acrylic acid;AA) copolymer fiber impregnated with platinum undergoes reversible shrinkage in a 1% NaCl solution when the polarity of the fiber is changed from negative to positive [11]. They reasoned that the positively charged fiber, acting as anode, causes the following electrochemical reaction in and around the fiber:

$$2H_2O \rightarrow O_2 + 4H^+ + 4e^-. \tag{1}$$

As the pH of the solution is lowered, the degree of dissociation of the carboxylic acid groups is low, and the polymer shrinks. When the fiber is again made negatively charged, it swells in response to the increased pH brought about by the following reaction:

$$4H_2O + 4e^- \rightarrow 2H_2 + 4OH^-. \tag{2}$$

Similar observations were published by De Rossi *et al.* [12]. They also worked with thin strips of PVA-PAA copolymer, immersed in a fluid bath between two platinum electrodes. The gels were fixed on one side and connected to a force transducer on the other, and data was taken of both isometric force generation and isotonic equilibrium length of the hydrogel under different conditions. They found that the response of the hydrogel strips under electric stimulus is very similar to the response when only the pH of the fluid medium is changed and no electric field is applied. When a potential is applied to the electrodes, an acid front propagates away from the anode by diffusion, as does a base front from the cathode. In De Rossi's experiment, the hydrogel membrane was positioned much closer to the anode than the cathode, and therefore shrank in response to the acid front.

Shiga and Kurauchi reported a different deformation of a hydrogel in an electric field. They found that a poly(sodium acrylate; AANa) gel placed in a NaOH solution between two electrodes (but not touching them) swells at the anode side when an electric field is applied [9]. In subsequent experiments Shiga observed even more complex behavior. First, he looked at a PAANa gel in four different fluidic media, touching the anode in all cases. When an electric field was applied, each hydrogel sample shrank at the anode, regardless of the surrounding fluid (aqueous HCl, NaCl, and NaOH solutions, and water). These results are consistent with the behavior seen by Hamlen and De Rossi. However, when each hydrogel sample was moved *away* from the anode, different responses were seen. In HCl and NaOH solutions, the anode side of the gel swelled in response to an applied electric field, in water, the PAANa gel contracted, and in the aqueous NaCl solution, the gel initially expanded but after a certain amount of time shrank.

The swelling behavior of PAANa and other hydrogels has been explained as being induced by a change in osmotic pressure based upon a difference in mobile ion concentrations between the inside and the outside of the gel [9], [13]. In the following section, a model is presented that uses this mechanism as a starting point to determine the swelling and deswelling kinetics of electrically triggered hydrogels.

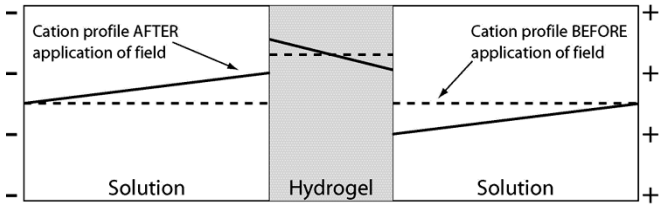

Fig. 1. Cationic concentration profile before and after application of an electric field. Before application, the concentration of cations inside the anionic gel is higher than in the external bath. Once a field is applied, cations inside the hydrogel are drawn to the cathode. At the hydrogel-solution interfaces, cations are either drawn into (anode side) or expelled from (cathode side) the hydrogel, thereby lowering or raising the concentration in the surrounding fluid. The cations considered are assumed not to undergo electrochemical changes at the electrodes, and therefore the concentrations at the electrodes remain more or less constant.

Although most previous work has been done at larger scales, experiments have been carried out with hydrogel samples smaller than one millimeter. Kishi and Osada studied hydrogel particles of diameter 150–300 μm in an electric field, and found that the response time was greatly improved in comparison to larger gels [14]. According to their calculations, gels 1 μm in diameter would undergo 96% volume change in as little as 0.23 ms. This result underscores the potential of using electrically triggered hydrogels as fast acting valves or actuators in microfluidic systems.

B. Theory

Initial experiments with hydrogels in electric fields showed that fast, repeatable volume changes are possible by taking advantage of the osmotic pressure-based mechanism discussed earlier [15], [16]. This mechanism is driven by mobile ion concentration differences in and around a hydrogel in an aqueous solution. In the absence of an electric field, the distribution of ions follows the principle of Donnan equilibrium [17], whereby the ionic concentration inside a hydrogel membrane having fixed charges (i.e., acidic or basic groups bound to the polymer matrix) is not necessarily equal to the external bath concentration. For instance, if the hydrogel considered is anionic, the concentration of cations inside the gel is higher than in the surrounding bath and the concentration of anions is lower in the gel than in the bath before application of any electric field. Electroneutrality is maintained because of the fixed positive charges in the hydrogel matrix.

When an electric field is applied, mobile ions inside and outside the hydrogel are rearranged, and concentration gradients are established. The nature of these gradients is complex, but a general understanding can be arrived at by considering the simplified case of a hydrogel membrane spanning a fluid-filled channel. Fig. 1 shows the effect of an applied electric field on mobile cations in and around the anionic hydrogel membrane (a similar diagram could be drawn for mobile anions). It should be

noted that the acidic groups bound to the polymer chains are assumed to be immobile under an electric field [18], and therefore the concentration of the bound groups are considered constant and uniform inside the hydrogel. These fixed charges retard the migration of free ions inside the hydrogel to some extent. As a result, the ionic concentration gradient inside the gel is smaller than in the solution. The results presented by Wallmersperger *et al.* [19] and Doi *et al.* [13] show similar ionic concentration distribution upon application of an electric field. The hydrogels used in this report are cylindrical posts rather than membranes, which will complicate the reasoning in Fig. 1 somewhat. In addition, other experimental conditions such as flow and the creation of bubbles will affect ion migration, as well. Study of the simplified case, however, permits a basic understanding of mobile ion migration in and around the hydrogel.

For most of the experiments presented in this paper, the salt considered is K_2CO_3, which dissociates as follows:

$$K_2CO_3 \Rightarrow 2K^+ + CO_3^{2-}. \tag{3}$$

Hence, the concentration of mobile cations is twice the concentration of anions in solution. Fig. 1 shows, and calculations support, that the cationic concentration difference at the anode side of the hydrogel is larger than at the cathode side. As a result, the osmotic stress due to cations and the corresponding swelling should be greater at the anode side. The osmotic stress due to anion concentration gradients will be of lesser magnitude. It should be noted that the development of a pH gradient inside the hydrogel may also contribute to the deformation of an electrically triggered hydrogel because the composition and structure of these and pH-responsive hydrogels are the same [19].

According to Nemat–Nasser, the strain generated within an electroresponsive ionic polymer gel depends on "the relative influence of electrostatic and fluid-induced swelling forces" and their coupling effect, which in turn depends on the configuration of the gel with respect to the electrodes [20]. In an ionic polymer-metal composite (IPMC) consisting of a gel sandwiched between two electrodes, the electrostatic stress due to an imbalanced charge density dominates over the fluid-induced swelling forces (e.g., the osmotic stress). However, in an ionic hydrogel removed from the electrodes, the osmotic stress dominates over the electrostatic stress. When a salt solution is present between the hydrogel and the electrode, ions tend to migrate in such a way to minimize the net charge imbalance in the entire domain of the hydrogel and the solution [13]. The test devices presented in this paper are of the type in which a salt solution is present between the hydrogel and the electrodes. As a result, the magnitude of the osmotic stress is expected to be much larger than the electrostatic stress.

III. Model

A chemoelectromechanical model has been developed to predict the swelling and deswelling kinetics of hydrogels in response to an electric field, and is presented here.

The flux of the kth ionic species in the x-direction, Γ_{kx}, is described by the Nernst–Planck equation, which includes flux due to diffusion, electrical migration, and convection

$$\Gamma_{kx} = \phi\left[-\bar{D}_k\frac{\partial c_k}{\partial x} - \bar{\mu}_k z_k c_k \frac{\partial \Psi}{\partial x}\right] + c_k U_x \tag{4}$$

where ϕ is the gel porosity, $\bar{D}_k$ is the effective diffusivity [21] of the kth ion inside the hydrogel, $c_k, \bar{\mu}_k$, and z_k are the concentration, ionic mobility, and valence of the kth ion, respectively, Ψ is the electric potential, and U_x is the fluid velocity in the x-direction. The Einstein relationship relates diffusivity to ionic mobility

$$\bar{D}_k = \frac{\mu_k RT}{F} \tag{5}$$

where R is the universal gas constant, T is the absolute temperature, and F is Faraday's constant. Gel porosity is a function of the hydration state of the gel

$$\phi = \frac{H}{1+H}. \tag{6}$$

H is defined as the ratio of the volume of the fluid to the volume of the solid in the gel [22]. The flux of the kth ionic species in the y-direction, Γ_{ky}, is analogous to the x-direction expression (4).

The two dimensional continuity equation for the gel is

$$\frac{\partial(Hc_k)}{\partial t} = -(1+H)\left[\frac{\partial \Gamma_{kx}}{\partial x} + \frac{\partial \Gamma_{ky}}{\partial y}\right], (k = 1, 2, \ldots, N) \tag{7}$$

for N ionic species considered. One way in which this model deviates from previous models (most notably [19]) is the special way in which hydrogen ions are considered. Some H^+ ions bind to charged groups inside the gel, and the continuity equation for H^+ is modified [23]

$$\frac{\partial}{\partial t}\left[Hc_H + Hc_H^b\right] = -(1+H)\left[\frac{\partial \Gamma_{kx}}{\partial x} + \frac{\partial \Gamma_{ky}}{\partial y}\right] \tag{8}$$

where c_H^b represents the bound H^+. Another modification that must be made for H^+ is taking into account the amount created from water at the anode. This is included in the model by making use of the first law of electrochemistry [24]. OH^- created at the cathode need not be considered because experimental flow conditions shall prevent any of it from entering the test area.

The electric field is computed by solving the 2-D Poisson equation

$$\frac{\partial^2 \Psi}{\partial x^2} + \frac{\partial^2 \Psi}{\partial y^2} = -\frac{F}{\epsilon\epsilon_0}\left(\sum_{k=1}^{N} z_k c_k + z_f c_f\right). \tag{9}$$

The mechanical deformation of the hydrogel occurs at a much faster rate than the diffusion processes of the mobile ions. As a result, the mechanical deformation of the hydrogel can be assumed to be occurring quasi-statically. The mechanical field, therefore, is given by

$$\nabla \cdot \sigma = 0 \tag{10}$$

where σ is the stress tensor. The various components of the stress tensor are given by the following expressions:

$$\sigma_{xx} = \frac{E}{(1+\nu)(1-2\nu)}\left[(1-\nu)\frac{\partial u_x}{\partial x} + \nu\frac{\partial u_y}{\partial y}\right] - (P_{\text{osmotic}} + \sigma_{\text{electrostatic}}) \tag{11}$$

$$\sigma_{yy} = \frac{E}{(1+\nu)(1-2\nu)}\left[(1-\nu)\frac{\partial u_y}{\partial y} + \nu\frac{\partial u_x}{\partial x}\right] - (P_{\text{osmotic}} + \sigma_{\text{electrostatic}}) \tag{12}$$

$$\tau_{xy} = \tau_{yx} = G\left[\frac{\partial u_x}{\partial y} + \frac{\partial u_y}{\partial x}\right]. \tag{13}$$

Here, E is Young's modulus, G is the shear modulus, and ν is Poisson's ratio. The components of the eigenstress [20] acting on the ionic polymer gel are the electrostatic stress and the osmotic pressure (i.e., the fluid induced stress) due to the difference in the ionic concentration inside and outside the hydrogel. The osmotic pressure is given by

$$P_{\text{osmotic}} = RT\sum_{k=1}^{N}(c_k - c_k^o). \tag{14}$$

where c_k^o represents the concentration of the kth ion outside of the hydrogel. The effect of electrostatic stress is found to be negligible compared to that of the osmotic stress. However, for completeness, the present model considers the electrostatic stress in the following way [20]:

$$\sigma_{\text{electrostatic}} = k_0\nabla\cdot(k_e\nabla\Psi)\begin{bmatrix}1 & 0\\ 0 & 1\end{bmatrix} \tag{15}$$

where k_0 is a material property dependent on polymer geometry and fixed charge distribution, and k_e is the effective dielectric constant of the polymer.

Our model for electrically triggered hydrogels takes into account the variation of Young's modulus with both hydration and applied electric field, this being another point of deviation from previously proposed models. The variation of Young's modulus with changing hydration is given by the following model [25]:

$$E = E_0\frac{(1+H_0)^{1/3}}{(1+H)^{1/3}}. \tag{16}$$

Here, E_0 is the initial modulus and H_0 is the initial hydration of the gel.

The effect of applied electric field on Young's modulus is taken into consideration by the following model [9]:

$$\Delta G = \left(\frac{9}{4}\right)C\epsilon_1\epsilon_0\kappa^2E_f^2 \tag{17}$$

where ΔG is the change in the shear modulus, C is the volume fraction of the charged polymer matrix (i.e., $C = (1+H)^{-1}$), E_f is the electric field, and κ is the Clausius–Mossotti function [26], which is a function of the relative dielectric constant of the solvent and that of the polymer matrix. The change in Young's modulus, ΔE, can be related to the change in the shear modulus, ΔG, by the following expression:

$$\Delta E = \frac{\Delta G}{2(1+\nu)}. \tag{18}$$

The coupled chemical, electrical, and mechanical equations presented in this section cannot be solved analytically. The Finite Cloud Method [27], [28] is used to solve the governing equations numerically.

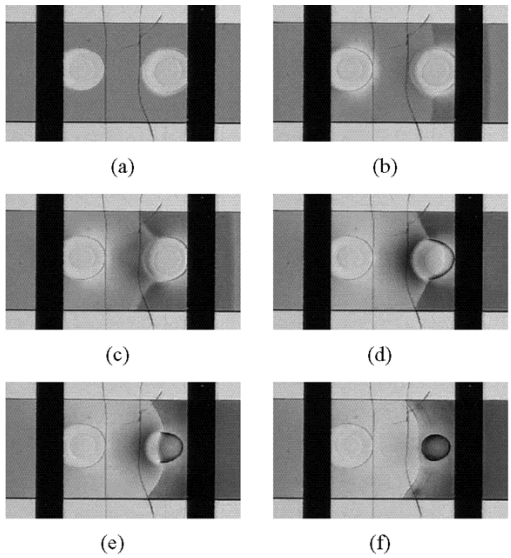

Fig. 2. Images of hydrogels under low dc voltage, no flow conditions. At 0 s, 3 V is applied to the electrodes (anode on the right). The channel is filled with DI containing Bogens universal indicator, which is red at pH less than 4, yellow at pH 4–6, green at pH 6–9, and blue at higher pH (all pH ranges approximate). As time progresses, a low pH front diffuses away from the anode, while a high pH front leaves the cathode. The hydrogel on the right shrinks in response to the acidic fluid surrounding it, while the hydrogel on the left, already fully swollen at pH 7, does not show any significant change. For scale reference, the electrodes are 500 μm wide.

IV. Fabrication

To create a test device that is inexpensive, simple to fabricate, and allows rapid design iterations, the μFT construction platform is chosen [1]. For the current experiments, a substrate with platinum electrodes patterned on top is required. This step is carried out with a standard microelectronics evaporation and etching procedure, but once finished, the addition of microfluidic channels and hydrogels is accomplished in less than 20 min.

To fabricate the substrate, a three-inch diameter quartz wafer is mechanically cleaned with acetone and isopropyl alcohol. On top of this is evaporated 2000 Å platinum with a 200 Å titanium adhesion layer. Photoresist is patterned to define the electrode geometry, the platinum is etched with an aqua regia solution (3:1 HCl:HNO_3 at 80 °C), and the titanium is removed with 1:2:7 HF:HNO_3:H_2O. To make electrical contacts, a conductive epoxy is used to connect small wires to platinum pads on the substrate.

Once the substrate is finished, channels and hydrogels are fabricated over the electrode structures. This task is completed quickly by following the μFT cartridge construction procedure: A polycarbonate cartridge (GRACE Bio-Labs HybriWell™) is placed on the substrate and filled with a photopolymerizable construction material consisting of isobornyl acrylate (IBA) and tetraethylene glycol dimethacrylate (9:1 weight ratio) and 2, 2-dimethoxy-2-phenyl-acetophenone (DMPA) (3.0 wt%). This liquid is exposed for 16 s (15 mW/cm^2) under a photomask that defines the channel geometry and hydrogel support posts.

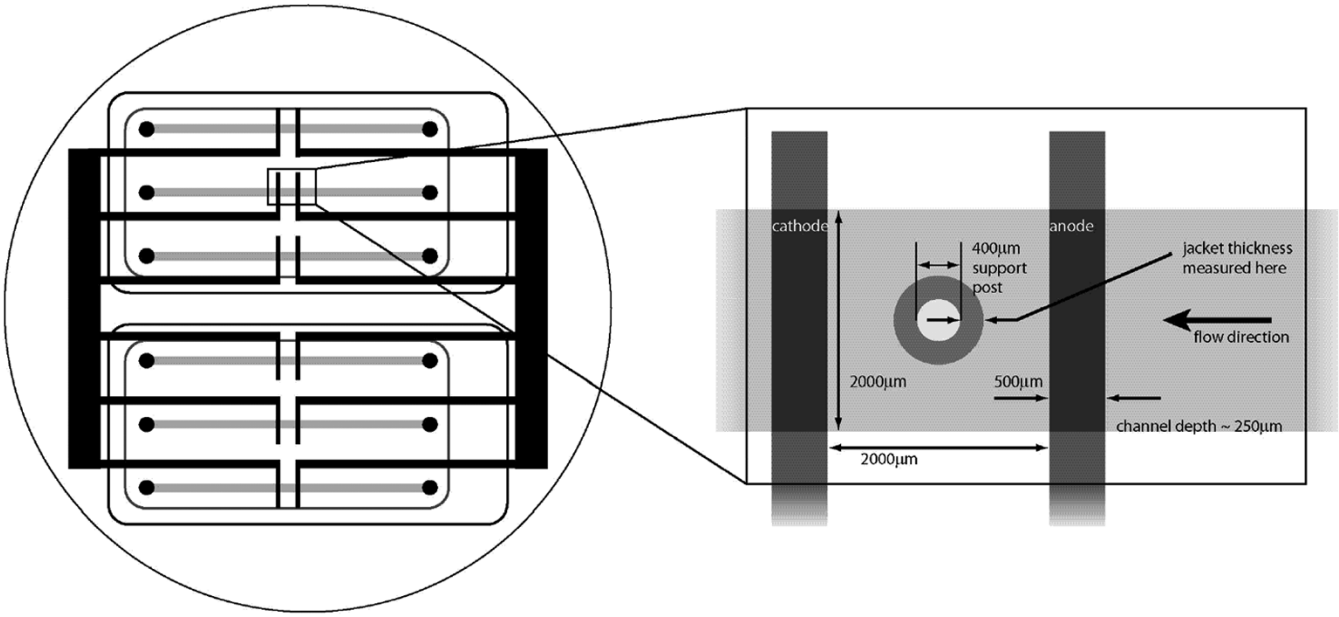

Fig. 3. Physical layout of the final test device. On the left is a representation of a metallized quartz substrate on top of which are two cartridge devices containing three microfluidic channels each. On the right, an expanded view of the test area. The channel is bounded by the polymerized construction material on the sides, the polycarbonate cartridge on top, and the quartz substrate with patterned platinum traces on the bottom. The support post is also made of construction material, and prevents the surrounding hydrogel material from moving or buckling.

The unpolymerized construction material is then driven out with an air gun and the channels flushed with methanol. Next, the active hydrogel jackets are fabricated in the channels by flowing in another pre-polymer mixture (AA and 2-hydroxyethyl methacrylate in a 1:4 molar ratio, ethylene glycol dimethacrylate [1.0 wt%], and DMPA [3.0 wt%]) and polymerizing (120 s, approx. 30 mW/cm2). The channel is flushed with methanol to remove the unpolymerized liquid, and the device is complete once press-on fluidic connectors have been attached. The connectors are made from PDMS, porous nitrocellulose material, and a double-sided adhesive, and allow flexible EVA tubing to be connected to the device with no leakage. See Fig. 3 for a visual representation of the finished device.

V. Results and Discussion

A. Hydrogel Under Low-Voltage, No-Flow Conditions

A simple method to trigger hydrogel volume change is to apply voltage to electrodes in the fluid medium surrounding the hydrogel. For water, an applied voltage of over 1.23 V should produce H^+ ions at the anode, thus lowering the local pH, and OH^- ions at the cathode, raising pH. Hydrogels placed near each electrode respond to these changes in pH (see Fig. 2). Of course, O_2 and H_2 gas is also produced, and if the solution is to remain free of bubbles, the amount of gas produced must be less than the respective solubility limits of each gas in water. The results seen in Fig. 2 are analogous to those seen by Hamlen *et al.* [11]. When the surrounding fluid is made acidic, the hydrogel shrinks. In a basic fluid medium, the hydrogel does not expand further, because in pH 7 water this particular hydrogel is already fully swollen (transition point of about pH 5 to 6).

B. Hydrogel Under Higher Voltage, No-Flow Conditions

With higher voltages, more complex behavior is seen. When voltage (more than about 5 V) is first applied, portions of the hydrogel nearest the anode begin to show rapid swelling. As time progresses, swelling continues across the gel until a moment is reached when swelling stops and shrinkage begins to occur. This brings to mind the results of Shiga [9], in which a PAANa hydrogel near the anode expanded initially in an aqueous NaCl solution, and after a time shrank. The swelling is the result of a change in osmotic pressure due to the electric field-induced migration of ions in and around the hydrogel. Within seconds of applying voltage, however, pH fronts created at the electrodes reach the hydrogels and then dominate the response, as in Fig. 2. In Shiga's experiment, an acid front created at the anode overtakes the gel and causes it to shrink.

C. Hydrogel Under Higher Voltage, Flow Conditions

To develop a high-speed electrically triggered hydrogel actuator, it would be advantageous to isolate the fast, osmotic pressure-based mechanism described in the previous section from the slower, pH-based mechanism. The simplest way to do this is by forcing fluid flow in the microchannel: ion migration inside the hydrogel is mostly unaffected while the H^+ and OH^- created at the electrodes is swept away by the flow. Additionally, the O_2 and H_2 gas created is also carried away. Doing this, hydrogels are free to continue their expansion due to ionic gradients and osmotic pressures, and are not affected by any bulk changes in fluidic pH. Initial tests with fluid flow were unsuccessful because gas bubbles were not effectively driven away by the flow. To remedy this, the completed device is placed in a 70 W, 50–100 mtorr oxygen plasma for 15 s. This step makes

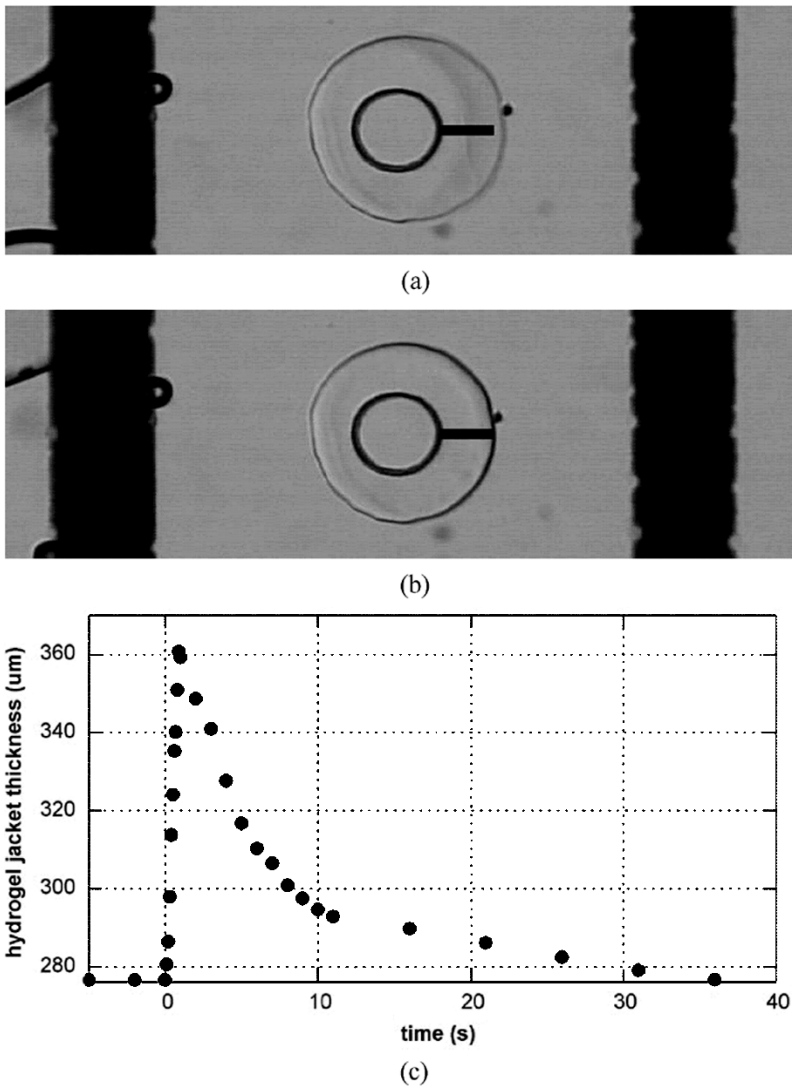

Fig. 4. Typical hydrogel response to applied dc voltage. At zero seconds, 23 V is applied to the electrodes, and the hydrogel jacket swells. After 1 s, the voltage is turned off, and after a time the hydrogel returns to its equilibrium jacket thickness. Scale bars are added for comparison purposes.

the channel less hydrophobic and prevents bubbles from adhering to the channel walls.

There are a number of parameters that must be controlled in carrying out an experiment with electrically triggered hydrogels. For instance, hydrogels respond to the same signal differently with variations in flow rate, flow direction (flows crossing the cathode first or anode first), location of the hydrogel in relation to the electrodes, fluid medium, temperature, and more. For the following experiment, several of these factors are kept constant across trials, and the effect of changing only one variable is observed. Fig. 3 shows the geometry of the test setup. The flow rate in the channel is constant at 0.5 ml/min (approximately 1.7 cm/s), the flow crosses the anode first, and the fluid medium is a pH 10 potassium buffer (SB116, Fisher Scientific, Fair Lawn, NJ). This buffer is used because we are interested in taking hydrogel response data in a fluid environment typical of that found in a microfluidic system used for biological applications. Before applying voltage, the channel is filled with the buffer and the hydrogel is allowed to equilibrate for approximately 15 min. After equilibration in the buffer solution, the device is connected to both a syringe pump and a dc voltage source. Under microscope, the response of the hydrogel jacket is observed and recorded for later analysis.

1) Typical Hydrogel Response: Fig. 4 shows a typical hydrogel response. The majority of shape change occurs in the portion of the hydrogel nearest the anode, as explained earlier, and it is in this region where all experimental data were collected. All data is expressed in μm measured from the inner edge of the hydrogel jacket (where the hydrogel and poly(IBA) post meet) to the outer edge.

2) Hydrogel Response to Different Applied Voltages: As the applied voltage is increased, there is an improvement in the time-response of the hydrogel expansion phase. Electric field intensities increase with higher applied voltage, and as a result, larger ion concentration gradients are established. This, in turn, leads to higher osmotic stress and more rapid swelling. The con-

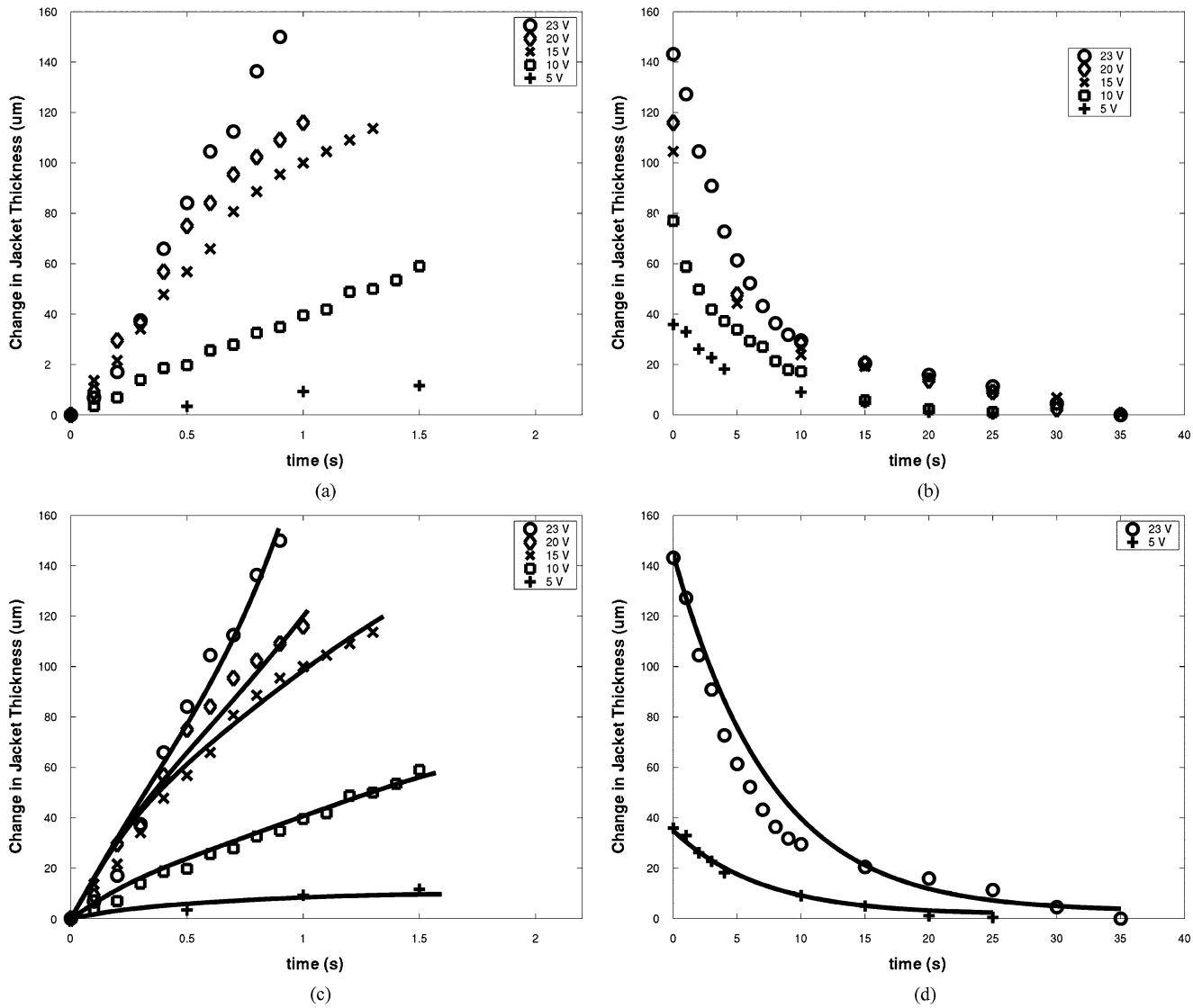

Fig. 5. Hydrogel response versus applied voltage. (a) At 0 s, voltage is applied to the electrodes. The speed of swelling increases as the applied voltage increases. (b) Hydrogel response when voltage is turned off (0 V at 0 s). For both plots, the vertical axis represents the change in hydrogel jacket thickness relative to the equilibrium thickness. (c) *and* (d) Simulation results superimposed on experimental data shown in (a) and (b), (a) swelling experimental, (b) deswelling experimental, (c) swelling simulation, and (d) deswelling simulation.

traction phase (all voltages equal zero) shows less of a dependence on the initial applied voltage (see Fig. 5). Although it may appear that a hydrogel swollen by a higher voltage contracts faster than a hydrogel subjected to a smaller initial voltage, this is not the case. Exponential curve fits given to the data show similar rates of decay. Please note that error bars in Fig. 5 and other subsequent figures are not shown because the data represents one trial only. This is primarily due to the fact that extracting the data from the video images is a highly labor-intensive process. More efficient methods of measuring hydrogel response are being developed and will be implemented in future work.

D. Hydrogel Subjected to Non-DC Voltage Waveforms

The primary drawback to using dc voltages to trigger hydrogel volume change is the fact that the gel continues to expand and will rupture if the voltage is not switched off. At higher voltages, this happens quickly, within 2 or 3 s at 20 V. At lower voltages (5 or 10 V), the hydrogel does not rupture as quickly, but the response time is not as good as with higher applied voltages. Ideally, we would like to be able to control a gel such that an equilibrium jacket thickness is reached quickly and held indefinitely. To accomplish this, a technique analogous to pulsewidth modulation (PWM) is used. A square wave signal with constant voltage amplitude and dc offset is applied, and only the duty cycle is altered to increase or decrease the hydrogel jacket thickness. Fig. 6 shows jacket thickness as a function of time for three different square wave voltage signals. These experiments show that, for constant amplitude signals, the equilibrium hydrogel volume is proportional to the duty cycle. As amplitude is increased, the speed of volume change (in transition between different duty cycles) is increased, as is the final equilibrium

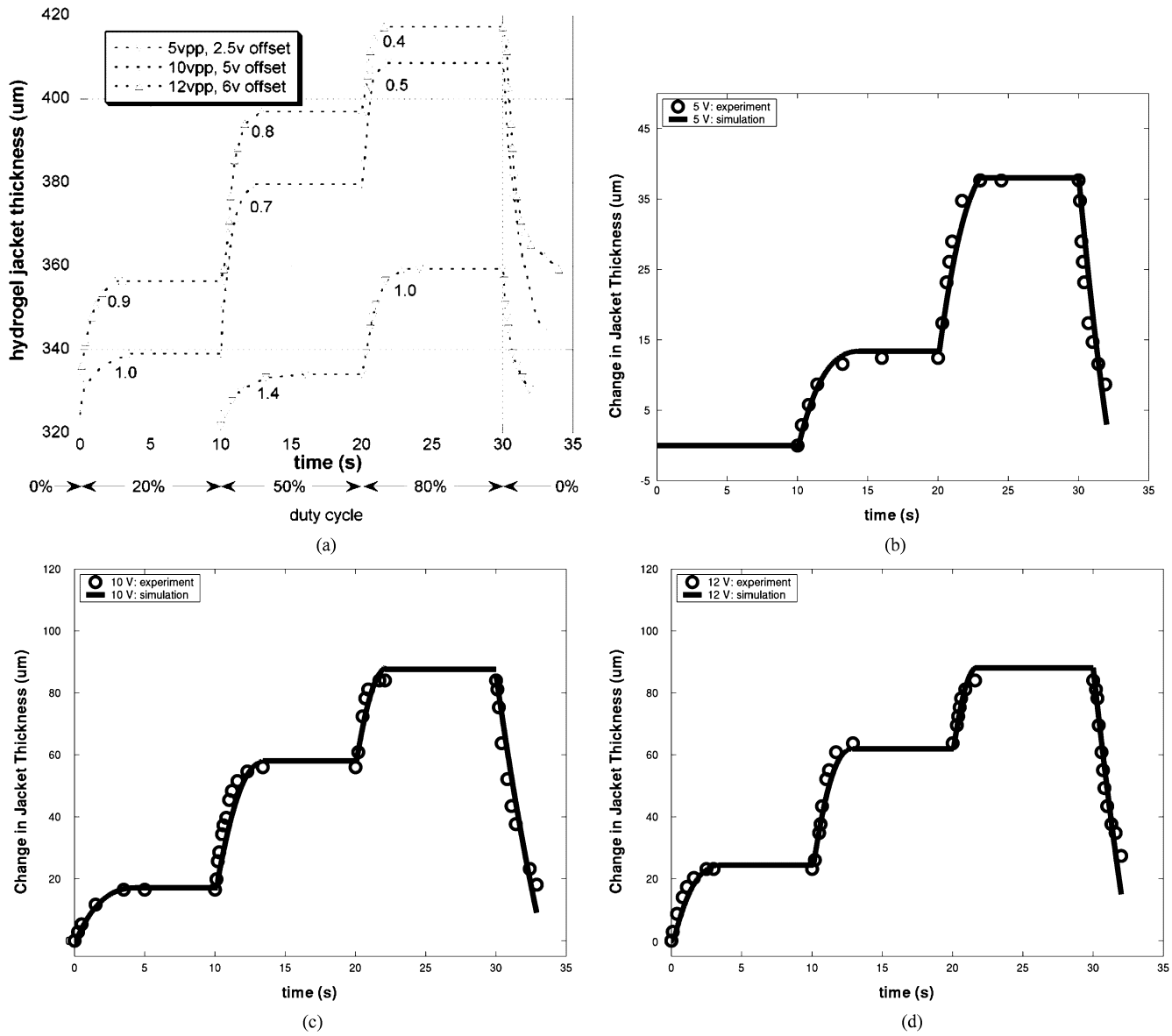

Fig. 6. (a) PWM experimental results. Before 0 s, the duty cycle of each square voltage waveform signal is 0% (0 dc volts). At 0 s, the duty cycle is raised to 20%, at 10 s, 50%, at 20 s, 80%, and then 0% again at 30 s. The numbers under each trace represent the rise time constants $(1 - 1/e)$ for each transition. (b) *through* (d) Simulation results for each data set shown in (a). Note: a 5 Vpp waveform at 20% duty cycle does produce a very small response. However, the equipment available did not allow collection of reliable data, (a) experimental results, (b) 5 V simulation, (c) 10 V simulation, and (d) 12 V simulation.

volume at higher duty cycles. Again, the hydrogel response is nonisotropic. Volume change is first observed nearest the anode (where jacket thickness is reported in Fig. 6) and then in areas further away from the anode.

E. Tailored Hydrogel Response

As noted earlier, changing hydrogel chemistry, fluid media, electrode configuration, and other system parameters could allow the potential for improved or tailored hydrogel response. The model presented in this paper has been shown to accurately predict hydrogel swelling and shrinking in response to an applied electric field, and could be a useful tool in designing systems that include electrically triggered hydrogels. As an example, Fig. 7 shows how changing the fixed charge concentration within a hydrogel matrix would theoretically alter its time-response.

VI. Conclusion

The results presented in this paper show that electrical triggering of hydrogel response could be a promising mode of control for high-speed valves and pumps in microfluidic applications. The time response of the volume change is much quicker than has been shown for other stimuli-responsive hydrogels, and the shape of the response can be tailored by engineering an appropriate electrical input signal. Pulse width modulated signals, for instance, are shown here to produce step responses, but with modification PWM could be used to create a steady ramp

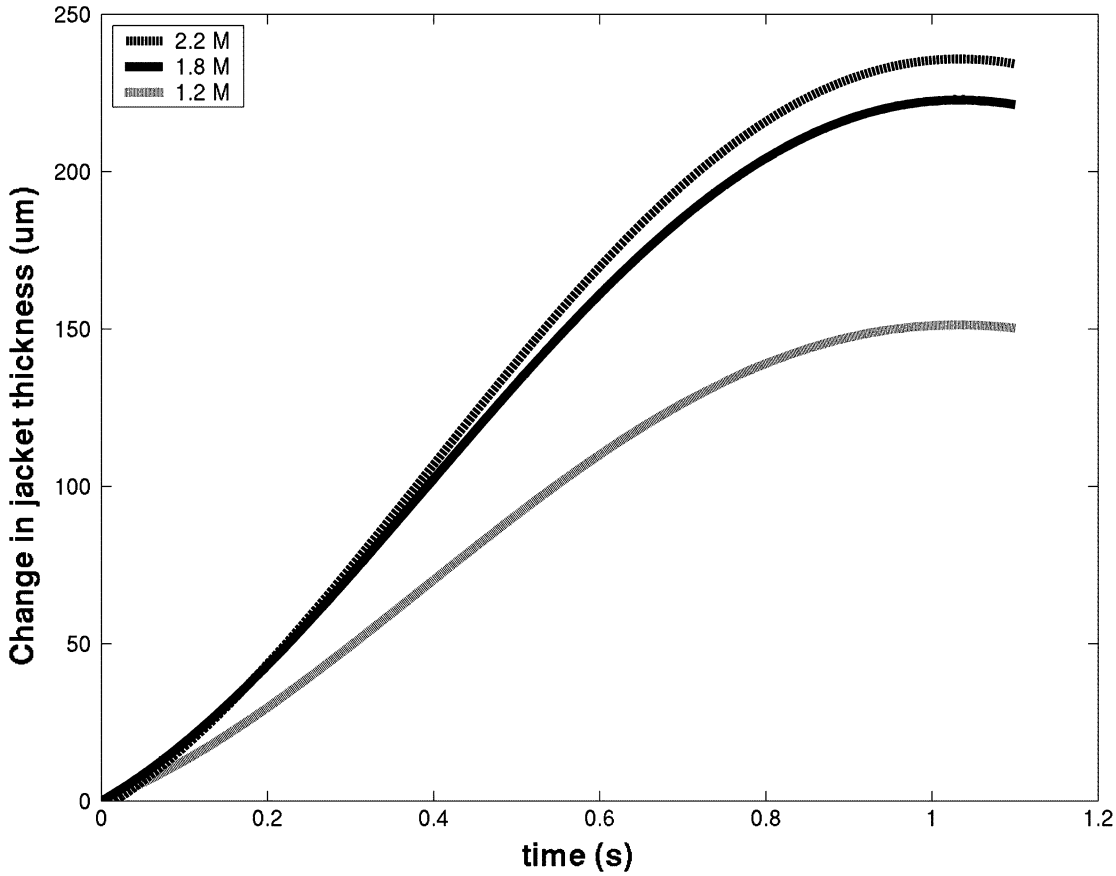

Fig. 7. The effect of fixed charge concentration on the swelling of a square shaped gel. The middle trace (1.8 M) represents the charge concentration of the hydrogels studied in the remainder of this paper.

response or a sinusoidal response, among others. In and of itself, having tight control of hydrogel volume is not very useful. The potential lies, however, with the incorporation of this mode of control into already proven microfluidic hydrogel devices. For instance, coupling an electrically triggered hydrogel with a membrane could make an effective throttle valve or active on/off valve. This configuration could also be used to create a micropump capable of dispensing small, discrete amounts of fluid. Several of these gels operated in cascade could act as a peristaltic micropump. Designing hydrogel filters with tunable porosity is another potential application. More complex electronic control schemes could make these gels useful in silicon-based microfluidic systems as well. Outside of microfluidics, there are several potential applications. Electrically triggered hydrogels are already used as muscle for robotics and artificial prostheses.

REFERENCES

[1] D. J. Beebe, J. S. Moore, Q. Yu, R. H. Liu, M. L. Kraft, B.-H. Jo, and C. Devadoss, "Microfluidic tectonics: A comprehensive construction platform for microfluidic systems," *Proc. Nat. Acad. Sci. USA*, vol. 97, pp. 13 488—13 493, 2000.

[2] J. C. McDonald and G. M. Whitesides, "Poly(dimethylsiloxane) as a material for fabricating microfluidic devices," *Accounts Chem. Res.*, vol. 35, pp. 491–499, 2002.

[3] D. J. Beebe, J. S. Moore, J. M. Bauer, Q. Yu, R. H. Liu, C. Devadoss, and B.-H. Jo, "Functional hydrogel structures for autonomous flow control inside microfluidic channels," *Nature*, vol. 404, pp. 588–590, 2000.

[4] T. Tanaka, I. Nishio, S.-T. Sun, and S. Ueno-Nishio, "Collapse of gels in an electric field," *Science*, vol. 218, pp. 467–469, 1982.

[5] A. Richter, D. Kuckling, S. Howitz, T. Gehring, and K.-F. Arndt, "Electronically controllable microvalves based on smart hydrogels: Magnitudes and potential applications," *J. Microelectromech. Syst.*, vol. 12, pp. 748–753, 2003.

[6] A. Suzuki and T. Tanaka, "Phase transition in polymer gels induced by visible light," *Nature*, vol. 346, pp. 345–347, 1990.

[7] K. Kataoka, H. Miyazaki, M. Bunya, T. Okano, and Y. Sakurai, "Totally synthetic polymer gels responding to external glucose concentration: Their preparation and application to on-off regulation of insulin release," *J. Amer. Chem. Soc.*, vol. 120, pp. 12 694–12 695, 1998.

[8] T. Miyata, N. Asami, and T. Uragami, "A reversibly antigen-responsive hydrogel," *Nature*, vol. 399, pp. 766–769, 1999.

[9] T. Shiga, "Deformation and viscoelastic behavior of polymer gels in electric fields," *Adv. Polymer Sci.*, vol. 134, pp. 131–163, 1997.

[10] Y. Osada and S. B. Ross-Murphy, "Intelligent gels," *Sci. Amer.*, pp. 82–87, 1993.

[11] R. P. Hamlen, C. E. Kent, and S. N. Shafer, "Electrolytically activated contractile polymer," *Nature*, vol. 206, pp. 1149–1150, 1965.

[12] D. E. De Rossi, P. Chiarelli, G. Buzzigoli, C. Domenici, and L. Lazzeri, "Contractile behavior of electrically activated mechanochemical polymer actuators," *Trans. American Soc. Artif. Intern. Organs*, vol. 32, pp. 157–162, 1986.

[13] M. Doi, M. Matsumoto, and Y. Hirose, "Deformation of ionic polymer gels by electric fields," *Macromolecules*, vol. 25, pp. 5504–5511, 1992.

[14] R. Kishi and Y. Osada, "Reversible volume change of microparticles in an electric field," *J. Chem. Soc., Faraday Trans. I*, vol. 85, pp. 655–662, 1989.

[15] M. J. Bassetti, J. S. Moore, and D. J. Beebe, "Development of electrically triggered hydrogels for microfluidic applications," in *Proc. 2nd Annual International IEEE-EMBS Special Topic Conference on Microtechnologies in Medicine and Biology*, 2002, pp. 410–413.

[16] M. J. Bassetti and D. J. Beebe, "Demonstration of hydrogel volume control using pulse width modulation," in *Proc. MicroTAS 2002 Symposium*, 2002, pp. 718–720.

[17] J. Malmuvio and R. Plonsey, *Bioelectromagnetism: Principles and Applications of Bioelectric and Biomagnetic Fields*. New York: Oxford University Press, 1995.
[18] Y. Hirose, G. Giannetti, J. Marquardt, and T. Tanaka, "Migration of ions and pH gradients in gels under stationary electric fields," *J. Phys. Soc. Japan*, vol. 61, pp. 4085–4097, 1992.
[19] T. Wallmersperger, B. Kroplin, J. Holdenreid, and R. W. Gulch, "A coupled multi-field-formulation for ionic polymer gels in electric fields," in *Proc. SPIE 8th Annual Symposium on Smart Structures and Materials*, vol. 4329, 2001, pp. 264–275.
[20] S. Nemat-Nasser and J. Y. Li, "Electro-mechanical response of ionic polymer metal composite," *J. Appl. Phys.*, vol. 87, pp. 3321–3331, 2000.
[21] J. S. Mackie and P. Meares, "The diffusion of electrolytes in a cation-exchange resin membrane ii. Experimental," *Proc. Royal Society, Series A: Mathematical and Physical Sciences*, vol. 232, pp. 510–518, 1955.
[22] S. K. De, N. R. Aluru, B. Johnson, W. C. Crone, D. J. Beebe, and J. S. Moore, "Equilibrium swelling and kinetics of pH-responsive hydrogels: Models, experimentation, and simulations," *J. Microelectromech. Syst.*, vol. 11, pp. 544–555, 2002.
[23] P. E. Grimshaw, "Electrical control of solute transport across polyelectrolyte membrane," Ph.D. dissertation, Massachusetts Institute of Technology, 1990.
[24] R. S. Berry, S. A. Rice, and J. Ross, *Phys. Chem.*. New York: Wiley, 2001.
[25] O. Okay and S. Durmaz, "Charge density dependence of elastic modulus of strong polyelectrolyte hydrogels," *Polymer J.*, vol. 43, pp. 1215–1221, 2002.
[26] T. B. Jones, *Electromechanics of Particles*. New York: Cambridge University Press, 1995.
[27] N. R. Aluru and G. Li, "Finite cloud method: A true meshless technique based on a fixed reproducing kernel approximation," *Int. J. Numer. Meth. Eng.*, vol. 50, pp. 2373–2410, 2001.
[28] X. Jin, G. Li, and N. R. Aluru, "On the equivalence between least squares and kernel approximations in meshless methods," *Comput. Model. Eng. Sci.*, vol. 2, pp. 447–462, 2001.

Michael J. Bassetti is working toward the Ph.D. degree in electrical engineering at the University of Wisconsin-Madison, where he received the M.S. degree in biomedical engineering in 2002. In 1998, he received the B.S. degree in electrical engineering from the University of Illinois at Urbana-Champaign.

He is currently with the Center for Nanotechnology under the direction of Prof. F. Cerrina, and is supported by the Genomic Sciences Training Program, which operates under a grant from the NIH/National Human Genome Research Institute. His research involves microfluidics, BioMEMS, DNA synthesis, and gene assembly.

Aveek N. Chatterjee received the B.Tech. degree in mechanical engineering from the Indian Institute of Technology (Kharagpur) in 2001 and the M.S. degree in mechanical engineering from the University of Illinois at Urbana-Champaign (UIUC) in 2003, with a minor in computational science and engineering. He is currently working toward the Ph.D. degree at UIUC.

His research interests include computational analysis and design of MEMS, Bio-MEMS and micro-TAS, numerical methods in engineering, computational micro/nanofluidics, and bionanotechnological systems.

N. R. Aluru (M'00) received the B.E. degree with honors and distinction from the Birla Institute of Technology and Science (BITS), Pilani, India, in 1989, the M.S. degree from Rensselaer Polytechnic Institute, Troy, NY, in 1991, and the Ph.D. degree from Stanford University, Stanford, CA, in 1995.

He is currently an Associate Professor in the Department of Mechanical and Industrial Engineering at the University og Illinois at Urbana-Champaign (UIUC). He is also affiliated with the Beckman Institute for Advanced Science and Technology, the Department of Electrical and Computer Engineering and the Bioengineering Department at UIUC. He was a Postdoctoral Associate at the Massachusetts Institute of Technology (MIT), Cambridge, from 1995 to 1997. In 1998, he joined the University of Illinois at Urbana-Champaign (UIUC) as an Assistant Professor.

Dr. Aluru received the NSF CAREER award and the NCSA faculty fellowship in 1999, the 2001 CMES Distinguished Young Author Award, the 2001 Xerox Award for Faculty Research, and the Willett Faculty Scholar Award in 2002. He is a Subject Editor for the IEEE/ASME JOURNAL OF MICROELECTROMECHANICAL SYSTEMS, Associate Editor for the IEEE TRANSACTIONS ON CIRCUITS AND SYSTEMS II, and serves on the Editorial Board of a number of other journals.

David J. Beebe (S'90–M'95) received the B.S., M.S., and Ph.D. degrees in electrical engineering from the University of Wisconsin-Madison in 1987, 1990, and 1994, respectively.

Currently, he is an Associate Professor in the Department of Biomedical Engineering at the University of Wisconsin-Madison. He is also a member of the UW Comprehensive Cancer Center, Vascular Biology Program, Stem Cell Program and Biotechnology Training Program. From 1996 to 1999, he was an Assistant Professor in the Department of Electrical and Computer Engineering and an Assistant Research Professor in the Beckman Institute for Advanced Science and Technology at the University of Illinois at Urbana-Champaign. From 1994 to 1996, he was an Assistant Professor at Louisiana Tech University. He From 1991 to 1994, he was an NIH Biotechnology Predoctoral Trainee. He has broad interests in biomedical instrumentation and the development and use of microfabricated devices for applications in medicine and for the study of biology. His current interests include technology development for the handling and analysis of biological objects, development of nontraditional autonomous microfluidic devices and systems, and the study of cell and embryo development in microenvironments.